Journal of Hazardous Materials, 11 (1985) 189—208
Elsevier Science Publishers B.V., Amsterdam — Printed in The Netherlands

AREA-AVERAGED CONCENTRATIONS, HEIGHT-SCALES AND MASS BALANCES

P.W.M. BRIGHTON

Safety and Reliability Directorate, UKAEA, Wigshaw Lane, Culcheth, Warrington, Cheshire WA3 4NE (Great Britain)

(Received May 10, 1984; accepted September 15, 1984)

Summary

The concentration data obtained in the trials without obstructions at Thorney Island are analysed to produce quantities relevant to box models of heavy gas dispersion. Mean concentrations are calculated by averaging horizontally over the cloud area. Results are plotted against a dimensionless time scaled using the initial area and buoyancy content. At early times, ground-level concentrations match a power-law dependence with index equal to the edge entrainment coefficient in a simple generic box model. Later the concentration decreases more rapidly as expected from the influence of top entrainment: this depends on a Richardson number involving the atmospheric turbulence. Simple functions are fitted to vertical concentration profiles to permit an integration over height. The time-variation of cloud height-scale and Richardson number are presented. Finally, the cloud mass balance is computed: the results appear reasonably self-consistent though various sources of systematic error can be detected particularly near the end of each trial.

1. Introduction

This paper is the second of a pair in which we aim to analyse the Thorney Island data to produce the quantities needed for comparison with integral models, often called "box models", of heavy gas dispersion. In [1], we have described ways of estimating the cloud area and the position of its centroid as functions of time. Here we turn to analysis of the digital concentration data itself in order to derive spatial averages of concentration and height-scales for the clouds. To assess the self-consistency of the analysis and to identify shortcomings we have also derived mass balances for the clouds, i.e. the ratio of the mass of gas apparently detected (according to our analysis) to that originally released. Before describing how we have attempted to obtain these in practice, it is first desirable to discuss how in principle we would like to define the quantities needed for comparison with box models.

In the discussion of box models, a dispersing cloud is usually pictured as a cylindrical shape within which the concentration is uniform. However, it is not necessary for their validity that the cloud should approximate to this

picture. They should be exactly valid if the cloud has any concentration distribution which is self-similar, i.e. the concentration distribution at one time can be made the same as that at any other time simply by rescaling the radius, the height and the concentration level. Mathematically, the concentration distribution is then of the form $c(r,z,t) = C(t)F(r/R(t), z/h(t))$ where r is horizontal distance from the axis of symmetry, z is height above the ground and t is time. R and h are the horizontal and vertical scales of the cloud. C is the scale for concentration and F is the dimensionless distribution function. This leaves open how C, R and h should be defined in a particular case. They can always be rescaled as long as F is suitably redefined.

A definition of R is already implicit in our first paper [1]. In the initial stages of the releases, visual records show a sharp edge to the smoke-marked cloud and gas sensors respond to the arrival of gas by a very rapid increase in concentration: the cloud outline is easily defined in these circumstances. Sideviews of the clouds show a fairly distinct top so that a height can be determined. This height has been used for fitting box models to data from the Porton trials [2]. However, the clouds achieve this height only in the annular gravity current head at its edge [3] and so it must be an over-estimate of the mean height of the cloud boundary. In the later stages of the releases a more careful definition is desirable. We expect the edges of the cloud to become fuzzy through the diffusive action of turbulence: taking the Gaussian concentration distribution literally, one must consider the cloud to occupy all space.

In principle, it is reasonable to define the cloud boundary as that surface of constant concentration which contains some fixed proportion of the total gas released. In the case of single instantaneous releases, however, the constant-concentration surfaces may be highly convoluted, multiply connected and fragmented because of the turbulent fluctuations. The cloud boundary calculated by box models corresponds to some kind of average, presumably an ensemble average over a large number of releases into the same mean flow conditions. (This raises the question of appropriate averaging times to define the mean atmospheric conditions — a question not yet fully resolved in principle [4].) This boundary of course would not be the right-circular cylinder of the box models but would have a height varying continuously from centre to edge. One might specify the cylinder by matching its area and volume to the ground area and volume of the real cloud boundary, defining the mean concentration C to conserve the mass of contaminant in the cloud. (Note that this concentration would be larger than the mean concentration in the cloud inside the ensemble-average boundary.) This method of matching a real cloud to a box model does not in fact involve the principle of self-similarity: indeed it is the aim of box modellers to describe non-self-similar situations, if only approximately.

In practice, one is faced with only one release in each set of conditions and the analysis must frankly be based on a hope that these individual realisations are not too remote from the ensemble mean. Several features of the data encourage us in this hope:

(i) The buoyancy-driven slumping leads to a visual cloud outline on the ground which does not depart wildly from a smooth shape. This can be contrasted with the highly irregular shape of passive releases such as Trial 4 on Thorney Island.

(ii) Our analysis of cloud advection [1] has used a straight path. The fact that it accounts reasonably well for the arrival and departure of gas at the sensor masts in most trials indicates that the erratic drifting of clouds due to large-scale lateral velocity fluctuations is not a serious problem. As discussed by Chatwin [4], such bodily advection of a cloud has a drastic effect on ensemble mean values. In any case, for instantaneous gas releases we would argue that it is relative diffusion that needs to be considered since hazard analysis is usually concerned with the consequences of a single release.

(iii) The values produced by the concentration sensors are already averages over small intervals of space and time, which are much smaller than the length- and time-scales of the cloud as a whole. The ground-level concentration records show a relatively low degree of fluctuation around the trend on the time-scale of the passage of the cloud past the sensor. At higher levels, this is not true — a high degree of intermittency is visible in many concentration records, with the peaks from the sensors on the same mast being highly correlated [5]. Thus it appears that turbulent fluctuations have a considerably greater effect on the local height-scale of the concentration profile than on its ground-level values.

We conclude from all this that the cloud path and outline as determined in [1] should be reasonable estimates of ensemble-mean quantities, certainly within the experimental error. Unfortunately, this cloud outline does not conform to the ideal definition given above because it depends on the sensitivity of the gas sensors to low concentrations, which is somewhat lower than 0.1% as noted in [1].

We have outlined what in principle we would like to obtain from the data and have argued that the actual experiments go some way to meeting the need for ensemble mean values. We now describe what can be achieved in practice. As well as extracting the relevant quantities from individual trials, we show that by comparing them through a suitable scaling of the results several of the elements of current box models seem to be confirmed.

2. Analysis of mean concentrations and related quantities

2.1 The method of horizontal averaging

The basic idea on which our analysis rests is to perform horizontal averaging over those sensors within the cloud outline on the ground at a particular time. While the horizontal extent of the cloud seems fairly well defined [1], the vertical structure remains to be determined.

The data were first read from magnetic tape and translated into the appropriate machine-code numbers. They were compacted by applying averaging over one-second windows; this averaging time is small enough to retain

the essential structure of the concentration records from the standard gas sensors [5]. The data were further compacted in order to economise on disc space by storing concentration values only between the arrival and departure times of the gas at each mast, which were determined in the course of the cloud envelope analysis [1]. These arrival and departure times, which are based on visual inspection of the ground-level concentration records, are listed in [6] for all the Phase I trials.

Horizontal averages were then calculated every second simply as an arithmetic mean of all the standard gas sensor readings in a particular height range for which the time was between the arrival and departure times for that mast. In all the trials from No. 7 onwards, the majority of sensors were located at standard heights of 0.4 m (i.e. ground-level), 2.4 m, 4.4 m and 6.4 m. Where sensors are located at other heights, the readings were included in the average at the nearest standard height. Sensors equidistant from the two nearest heights were allocated to the average at the lower of the two. On some masts, higher sensors did not detect gas at any time during the passage of the cloud and the concentration records were set to zero during validation [7]; these were included in the averages. On the other hand sensors that were not functioning were excluded.

No attempt was made to weight the concentration readings according to the vicinity of the edge of the cloud, as one might have done by analogy with numerical integration schemes. The set of masts in the cloud was regarded as giving an essentially random sample of concentrations within it. Over a period of time there should be no systematic bias towards sampling unrepresentative parts of the cloud since the masts are fairly uniformly spaced and they make traverses through the cloud as it moves past. Hence it is believed that nothing more sophisticated than a simple arithmetic mean is warranted. It is important to note that this averaging procedure is *not* dependent on particular estimates of the cloud outline such as those described in [1].

In trials 17, 18 and 19 there was a line of ground-level sensors deployed along the centreline of the array at 10 m intervals from the source up to 100 m. Of these, only those located on masts at 50 m and 100 m were used in the averaging procedure in order to avoid an excessive bias to a small part of the cloud. These two positions corresponded to sensor locations in other trials.

Figure 1 shows the results of this procedure at 1 s intervals for the first 200 s of trial 16. The results at ground-level are encouragingly smooth despite the short averaging time and the spiky nature of the start of most concentration records. The cloud first reaches a mast 12 s after release and the number of masts in the cloud gradually rises to a maximum of 7 which is briefly attained at 117 s. The number of masts then steadily decreases to 2 at 200 s with the gas leaving the last mast at 260 s.

At the higher levels the mean concentrations are more erratic, an effect magnified by the logarithmic scale in Fig. 1, but reflecting the intermittent

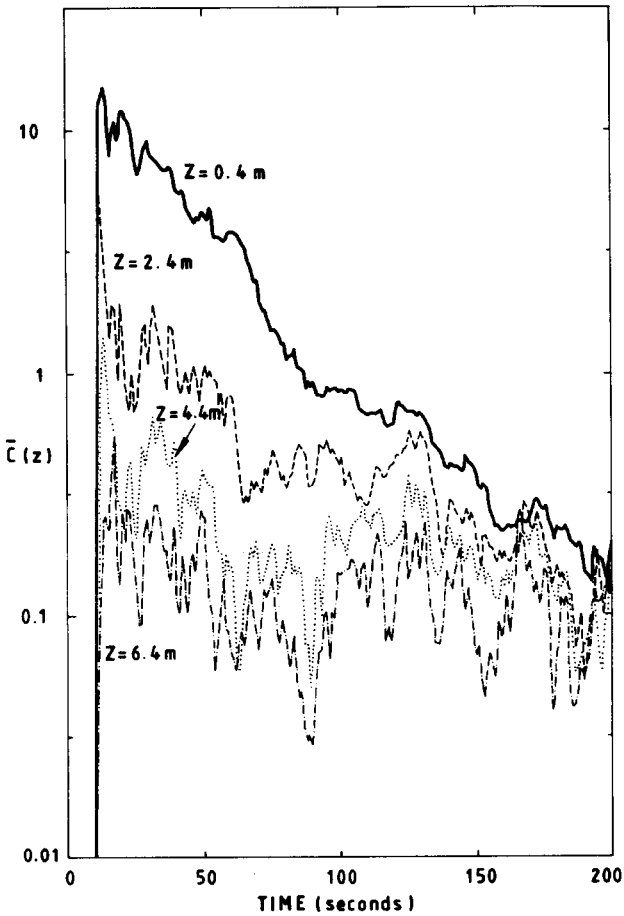

Fig. 1. Examples of horizontal concentration averages from Trial 16. 1-second averages. Heights indicated on graphs.

nature of the individual concentrations records. Nevertheless a steady decrease of concentration with height can be seen: the traces for different levels converge as time progresses implying a growth in cloud height.

Figure 1 is shown simply to illustrate the nature of the raw values of the area averaged concentrations. Results from other trials were of similar quality. To make valid comparison of results from different trials, replotting in a rescaled and smoothed form is needed as discussed in the following sections.

2.2. The scaling of the results: implications of box models

In order to appreciate the results for the mean concentrations, it is very helpful to consider the implications of a generalised simple box model of heavy gas dispersion. This indicates a useful non-dimensionalisation to apply to the timescale and gives some semi-quantitative predictions which can be compared with the experimental results.

The model is generalised in the sense that it reduces for specific parameter values to most of the models reviewed by Webber [8]. It consists of just two differential equations: the front condition is

$$U_F = dR/dt = Kb^{1/2}/R \tag{1}$$

where U_F is the front speed, K the frontal Froude number, with value 1.05 according to [1], and b the total buoyancy in the cloud which remains constant throughout the release for isothermal conditions, as at Thorney Island. The buoyancy is defined as

$$b = g\Delta' hR^2 \tag{2}$$

with

$$\Delta' = (\rho - \rho_A)/\rho_A$$

where g is the acceleration due to gravity, ρ is the cloud density and ρ_A is the ambient air density.

The second equation describes entrainment into the cloud:

$$dV/dt = 2\pi hRU_E + \pi R^2 U_T. \tag{3}$$

Here V is the cloud volume. The edge entrainment velocity is taken as

$$U_E = \alpha_E U_F \tag{4}$$

and the top entrainment velocity as

$$U_T = \alpha_T R\bar{i}^{-\mu} w'. \tag{5}$$

α_E and α_T are the dimensionless edge and top entrainment coefficients and w' a velocity scale for the atmospheric turbulence, which we choose to take as the r.m.s. value of the vertical wind component. Equation (5) includes a factor varying inversely with the Richardson number to represent the suppression of turbulence by the stable stratification of the gas cloud. The index μ is believed to be between 1 and 1.5 on the basis of laboratory experiments [9]. We define the Richardson number as

$$Ri = g\int_0^\infty \overline{\Delta'_m} dz/w'^2 = b/R^2 w'^2 = (R_0/R)^2 Ri_0. \tag{6}$$

In the first expression the subscript m denotes measured point values of Δ' and the overbar denotes the horizontal averaging process of Section 2.1 — this is used to determine the values of Ri presented in Section 2.5. The other two expressions are the form of Ri in the box model idealisation. Subscript 0 denotes release conditions. Note that Ri is unaffected by purely vertical mixing — it can be changed only by horizontal spreading of the cloud. Thus in the box model it is inversely proportional to cloud area.

These box-model equations are easily solved to yield the gravity-spreading law

$$(R/R_0)^2 = \tau = 2Kb^{1/2}(t - t_1)/R_0^2 \tag{7}$$

Here τ is the dimensionless time defined in eqn. (18) of [1] with t_1 the effective time origin for the linear area growth law. The entrainment equation gives

$$V/V_0 = (1 - \gamma)\tau^{\alpha_E} + \gamma\tau^{\mu + 2} \tag{8}$$

with

$$\gamma = [\alpha_T/2K(2 + \mu - \alpha_E)]\, Ri_0^{-\mu - \frac{1}{2}}(h_0/R_0)^{-1}.$$

The volume ratio V/V_0 is just the inverse of the concentration ratio C/C_0. The time-dependence of the Richardson number is

$$Ri = \tau^{-1}\, Ri_0. \tag{9}$$

For the Thorney Island Trials the parameter γ is found to be very much less than one by taking typical values of the model constants. This gives the interesting conclusion that for times τ that are not too large, eqn. (8) becomes

$$C/C_0 \approx \tau^{-\alpha_E} \tag{10}$$

On a log—log plot of concentration against τ the results for all trials should collapse on a single straight line of slope $-\alpha_E$ through the initial point $C/C_0 = 1$, $\tau = 1$. For sufficiently large times the top entrainment term of (8) will dominate giving

$$C/C_0 \propto \tau^{-(\mu + 2)}, \tag{11}$$

a much steeper line on the log—log plot. The time at which this behaviour will set in should increase as the initial Richardson number Ri_0 increases.
These heavy gas models remain applicable only as long as the top entrainment velocity (5) remains less than the value expected in passive dispersion. This condition breaks down at times of order Ri_0 when $Ri = O(1)$: thereafter passive dispersion is used to predict cloud behaviour.

2.3 Mean ground-level concentrations

In this section the key results of the paper are presented. These are graphs of mean ground-level concentration in the form suggested by the considerations of Section 2.2.

Table 1 lists the initial Richardson numbers based on values of the r.m.s. vertical wind component w' as calculated by NMI Ltd. from the ultrasonic anemometer at 10 m on the meteorological mast [10]. There are two trials with Ri_0 around 10^4 and then a fairly uniform spectrum of values from 2000 down to 200. The effective time origin t_1 is found from the graphs of area against time produced by the visual analysis [1,11]. For Trial 12 an estimate was used since there was no airborne coverage. The timescale $\mathcal{T}$ is calculated from eqn. (18) of [1]: where a reliable value of dA/dt was obtained from the visual records this is used. Otherwise (in Trials 5,6,12,13 and 17) $\mathcal{T}$ is

TABLE 1

Initial Richardson numbers, time-scales and extent of concentration measurements in Phase I trials

Trial no.	Ri_0	t_1 (s)	$\mathcal{T}$ (s)	Max. no. of masts in cloud	Duration of conc. measurements (s)
9	1.55×10^4	5	0.3207	22	>1200
12	8.32×10^3	5[a]	0.2507	23	>1000
17	1.86×10^3	4	0.1757	9	379
10	1.69×10^3	5	0.3110	4	224
8	1.63×10^3	8	0.3275	11	469
7	1.09×10^3	5	0.3683	9	380
6	993	3	0.4208	[b]	
19	751	3	0.2715	10	247
16	572	3	0.3957	7	260
13	559	5	0.2934	7	170
11	485	6	0.3361	7	181
5	391	5	0.3488	[b]	
14	346	6	0.4105	9	184
18	294	2.4	0.3311	8	137
15	219	2.3	0.4737	5	233

[a] Estimated: no airborne visual coverage.
[b] Results not available at time of writing.

calculated from the initial buoyancy obtained from the initial conditions listed in Table 1 of [1]. The values of Ri_0 in Table 1 use values of b consistent with the listed values of $\mathcal{T}$. In these calculations a value $K = 1.07$ was used based on the 7 trials totally unaffected by invisibility against the runway in Table 1 of [1].

To gauge the extent of the databases on which our average concentration values are based, Table 1 also lists the maximum number of masts in the cloud at any one time and the time at which gas left the last sensor. The Richardson number generally increases as the mean windspeed decreases and so at high Ri_0 the cloud spreads much more extensively while still within the sensor array. In Trials 9 and 12 sensors were still detecting gas when collection of data ceased.

Graphs of mean ground-level concentrations $\bar{c}_g$ against τ are presented in Fig. 2. To aid clarity of presentation the results at 1-second intervals, as illustrated in Fig. 1, have been smoothed using a moving average of the type recommended by Kendall [12]. This involves fitting a cubic curve to the data over a 15-second period centred on the time of interest — in producing the smoothed value at that time this procedure leads to a moving average with non-uniform weighting.

The results from the high-Ri_0 group of trials agree very well with the expectations raised in the last Section. In Fig. 2, a line $\bar{c}_g/C_0 = \tau^{-0.7}$ has been

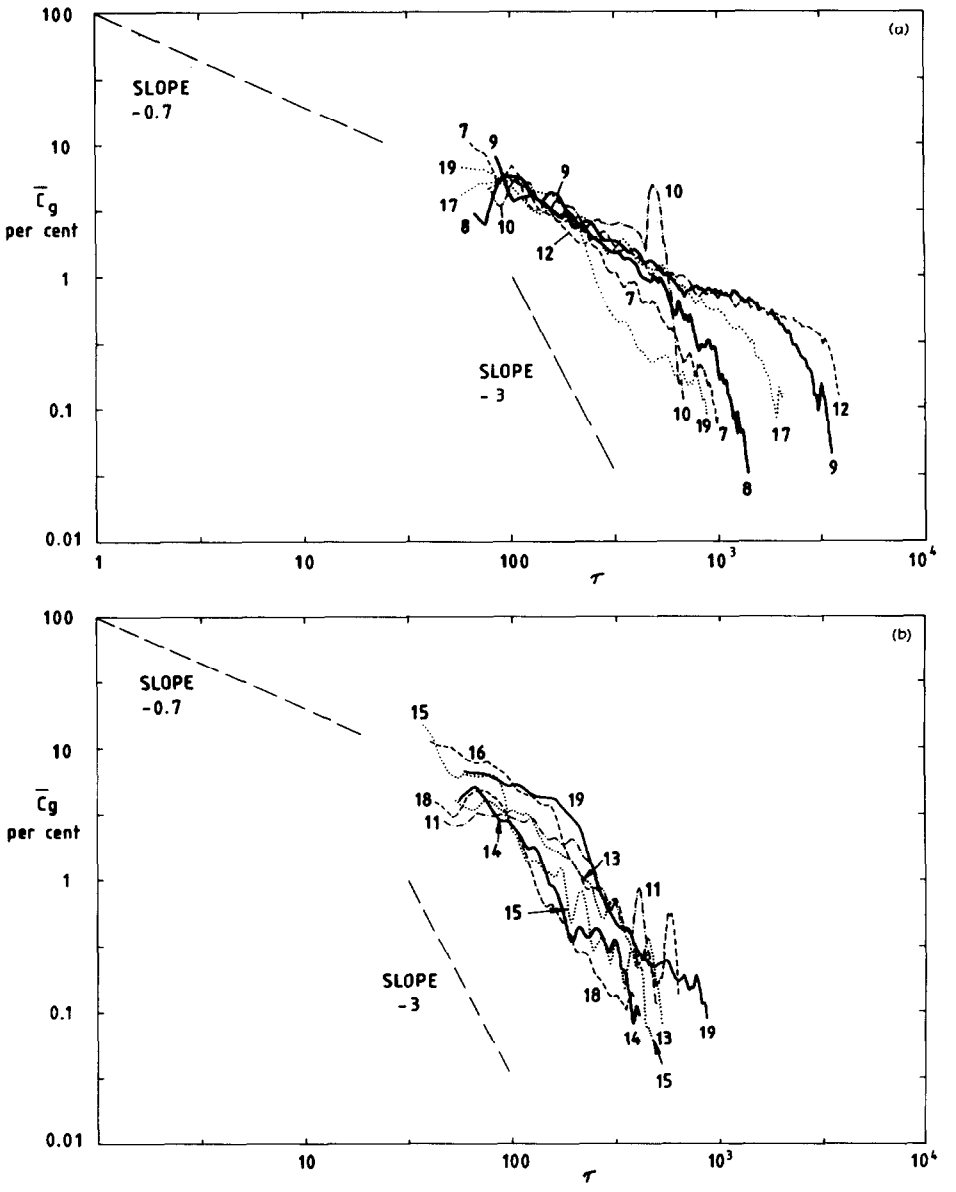

Fig. 2. Values of mean ground-level concentrations plotted against dimensionless time, τ. Logarithmic scales. Results smoothed over 15 seconds. Trial numbers indicated on graphs.

drawn through the initial conditions in order to guide the eye. The results from Trials 9, 12 and 17 follow this trend closely apart from some scatter at the start when only a few sensors are contributing to the average. This tentative value of $\alpha_E = 0.7$ has merely been selected by eye but it is in the range

of values used in current box models [8]. Towards the end of each set of data the lines fall away more steeply, though not quite in order of increasing Richardson number. However, this final fall-off may not be significant as at these times the area of maximum concentration may have left the sensor array.

Trial 10 gives less satisfactory results but does match the other trials for some of the time. Only a very small amount of data were available here because of a last-minute change of wind direction. The pronounced peak at the end of the data in Fig. 2 comes from a single sensor — this does at least serve to indicate how far individual sensors may deviate from the mean.

At lower Richardson numbers the curves still remain close to the trend of the high-Ri_0 trials at the start of the data but fall off more rapidly at an earlier stage, in just about the order of the Richardson numbers listed in Table 1. A line of slope -3 has been inserted as predicted in Section 2.2 for the top entrainment phase with $\mu = 1$. This is not suggested as a recommended value but serves to show that the concentrations may well follow a decay rate in the expected range.

It can be concluded that these results offer a strong possibility that these data can be fitted by a model of the simple type outlined in the preceding Section. It should be borne in mind that more weight should be attached to the middle portions of these curves where the maximum number of sensors are contributing to the average and that the extremities of the curves depend just on one or two sensors. This point will be taken up in the concluding section: we will also discuss there the fact that we have studied ground-level concentrations here rather than volume-averaged concentrations.

2.4 Cloud height-scales

The results of the calculations of Section 2.1 are values of horizontally-averaged concentrations $\bar{c}(z)$ at four different heights. Here we describe how we have fitted these data with vertical profile functions in order to estimate cloud height-scales and vertical integrals of $\bar{c}(z)$.

For most of the trials, the vertical profile was represented by a Gaussian profile modified by the inclusion of a constant plateau near the ground:

$$\left.\begin{array}{ll} \bar{c}(z) = \bar{c}_g, & z < h_p, \\ \bar{c}_g \exp\left[-(z-h_p)^2/2\sigma_z^2\right], & z > h_p, \end{array}\right\} \tag{12}$$

where $\bar{c}_g$ is the ground-level mean concentration of Fig. 2, h_p is the height of the constant-concentration region and σ_z is the standard deviation of the Gaussian. Form [12] was chosen to explore the frequently expressed view that heavy gas clouds are topped by a relatively sharp interface and to provide continuity between this postulated form of profile and the pure Gaussian customarily applied to the later, passive stages of dispersion; Wheatley and Webber [9] have suggested using such a profile in a box model. The two parameters of the profile (12), h_p and σ_z, can easily be found in practice because $L(z) = [\ln \bar{c}_g/\bar{c}(z)]^{1/2}$ becomes a linear function of z. Denoting the

values of $L(z)$ at the three levels of the elevated gas sensors z_i, $i = 1, 2, 3$ by L_i, the fitting procedure was to take a straight line through (z_1, L_1) and the mean of (z_2, L_2) and (z_3, L_3). The slope of this line gives σ_z and its intersection with the constant plateau $L = 0$ gives the value of h_p.

In practice it was found in all the Phase I trials that for most of the time this procedure implied $h_p < 0$. Since this gives a profile with the wrong ground-level value, a simple Gaussian with $h_p = 0$ was used in these circumstances, and σ_z was determined from a line passing through $L = 0$ at $z = 0$ and through the mean of the three points (z_i, L_i). $\bar{c}_g$ was taken to apply at $z = 0$ m, rather than at the actual sensor height of 0.4 m, for computational convenience; in practice, this makes a difference of less than 1% to the estimate of σ_z. In some trials there were a few times at which the data were erroneous or in some other way did not fit this model. In cases where one of $\bar{c}_2$ and $\bar{c}_3$ was less than zero, that value was ignored (here $\bar{c}_i$ denotes $\bar{c}(z_i)$): this could occur if all the sensors at these levels registered only "noise" when the corresponding ground-level sensors were contributing to the averages. If $\bar{c}_1$ was greater than $\bar{c}_g$, then $\bar{c}_1$ was used as the ground-level concentration. With more severe difficulties such as $\bar{c}_2$ and $\bar{c}_3$ both less than zero or both greater than $\bar{c}_g$ and $\bar{c}_1$, the attempt to fit a vertical profile at that time was abandoned.

In Trials 9 and 12, with the highest initial Richardson numbers (see Table 1), the clouds were generally so low that virtually no gas was detected at the upper two levels of gas sensors and hence the Gaussian profiles could not be fitted. For these trials, the vertical concentration profiles were fitted by linear interpolation between the data points. The value $\bar{c}_g$ from the lowest level sensors was taken as applying at the actual height of 0.4 m.

Results of calculations using these procedures are illustrated by Fig. 3, where we show the estimate of the height at which the horizontally averaged concentration reaches 10% of its ground-level value (or its value at z_1 in the rare cases where this is greater) according to the profiles described above.

For the highest initial Richardson numbers, the height-scale rapidly drops to a level value when the concentration at $z_1 = 2.4$ m becomes much less than 0.1 $\bar{c}_g$. This must be regarded as an upper bound on the true value. In Trial 12 higher values are achieved again near the end of the recorded data.

For lower Ri_0, the graphs display a considerable degree of irregularity on a short time-scale. This is because of the sensitivity of the Gaussian profile to the fluctuations in the low concentrations recorded at the higher levels as illustrated in Fig. 1. In fact to reduce this variation, the height-scale plots of Fig. 3 have been obtained after smoothing the mean concentration values according to the procedure described in Section 2.3. The results show that the cloud height-scale is around 4—5 m for $\tau \approx 100$ when the data begin and then increases at a rate which increases with decreasing Richardson number. A the end of the data, the upward trend falters or even changes to a decrease in several of the trials; this is thought to be because the gas is becoming too dilute in the upper reaches of the clouds to be detected reliably.

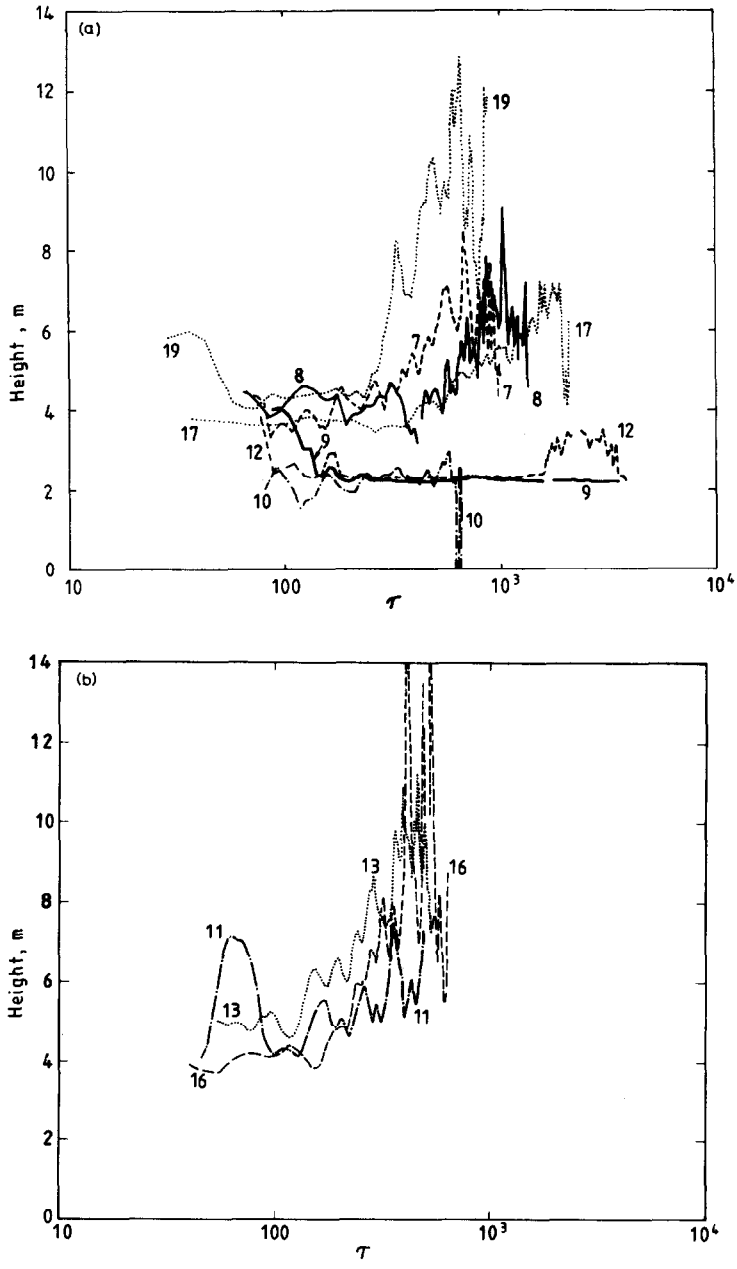

Fig. 3. Estimated heights to 10% ground-level concentration plotted against dimensionless time, τ. Calculated from mean concentrations smoothed over 15 seconds. Trial numbers indicated on graphs.

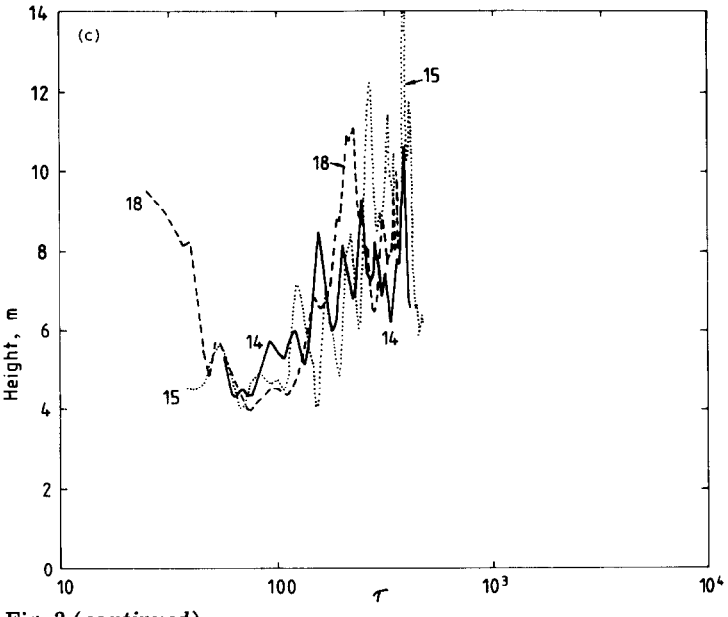

Fig. 3 (*continued*).

2.5 Richardson numbers

A cloud Richardson number based on horizontal averages of concentrations has been defined above in eqn. (6). It has been evaluated by integrating the modified Gaussian and linear concentration profiles which were fitted to the data to obtain the height-scales as described in Section 2.4.

Results are shown in Fig. 4. This includes lines of slope −1 through the values of the initial Richardson numbers given in Table 1. If the cloud spreads solely through gravity slumping, then Ri should be inversely proportional to time as in eqn. (9), being unaffected by vertical mixing. Thus this calculation of Ri provides an independent way of estimating cloud areas which may be compared to the results from the cloud envelope analysis of [1].

In practice the results do follow this expectation for much of the time though generally at a level slightly below the line through Ri_0. Also towards the end of the data there tends to be a decrease at a faster rate. In some cases this may be correlated with the anomalous decrease at the end of some of the height-scale graphs of Fig. 3, i.e. the vertical integral of concentration has probably been underestimated. In most of the trials Ri is less than 1 by the end, implying that the dispersion may have become passive. A more precise estimate of the transition to passive behaviour can be made only when values for the top entrainment parameters become available so that the entrainment velocity (5) can be compared with the passive value.

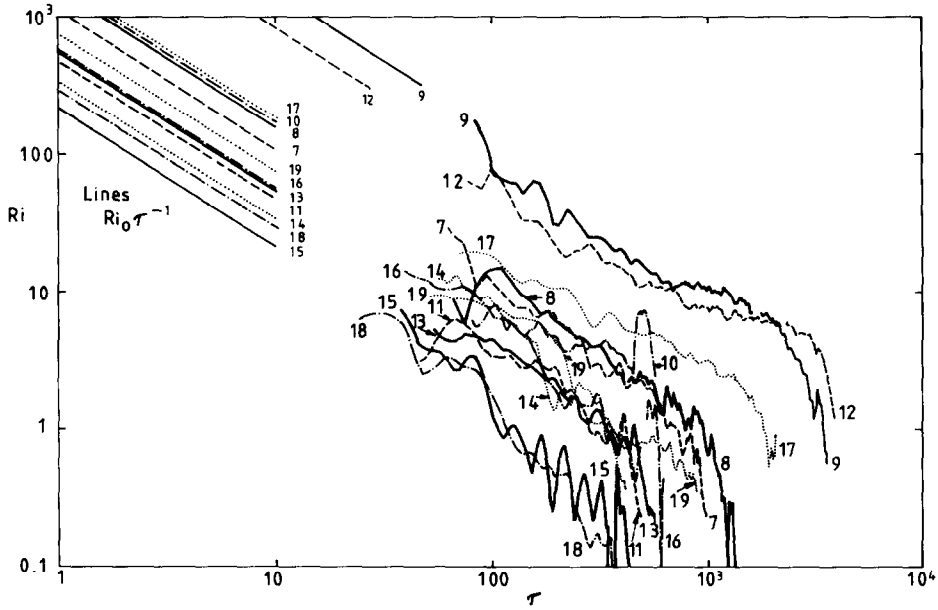

Fig. 4. Cloud Richardson numbers, $Ri = g\Delta'_0 \int_0^\infty \bar{c}(z)dz/c_0 w'^2$, plotted against dimensionless time, τ. Calculated from mean concentrations smoothed over 15 seconds. Trial numbers indicated on graphs.

2.6 The mass balance

The final quantity for which we wish to present estimates is the mass balance of the cloud. This is defined as

$$M = A\int_0^\infty \bar{c}(z)dz/V_0c_0, \tag{13}$$

where A is the cloud area V_0 is the inital cloud volume from Table 1 of [1] and c_0 is the initial concentration, which is 100% by definition. As for the Richardson numbers, the integral is calculated from the fitted profiles of Section 2.4. If the gas measurement and data analysis systems were perfect, M should always have the value 1, assuming no deposition or the like.

The results of the calculations are shown in Fig. 5. The area estimates are those presented in Fig. 8 of [1], which, over the period for which the concentration measurements are available, are based mainly on the cloud envelope analysis. As discussed in [1] and fully described for all Phase I trials in [6], there are usually several possible cloud envelopes because of the 100 m mast spacing. Those used have been selected partly to keep M closest to 1 overall. The results are discussed in descending order of Ri_0.

For Trials 9 and 12, a good match to the ideal $M = 1$ is achieved, with the largest deviations occurring at the beginning when there are few masts in the cloud and at the end when M drops below 0.5. It is interesting to note that this decrease occurs much later and more abruptly than the decrease in the normalised cloud area A/A_0 τ shown in Fig. 8 of [1]. On the other hand it

does match the sudden steepening at the ends of the mean ground-level concentration curves seen in Fig. 2. This does not necessarily invalidate the interpretation of the effect as due to top entrainment. An associated increase in height may have led to concentrations at the higher level sensors too low to detect. However it must be admitted that the good results for M here may be fortuitous because the vertical profiles for these clouds are particularly uncertain since almost all the gas appeared to lie below 2.4 m (see Section 2.4).

Similar remarks apply to the mass balance for Trials 17, 8 and 7 except that the modified Gaussian concentration profile could be used here and so the estimates of $\int_0^\infty \bar{c}(z)\mathrm{d}z$ should be more reliable. The fall-off in M at the end corresponds closely to the behaviour at the end of the height-scale graphs (Fig. 3).

The poor results for Trial 10 again reflect the paucity of data on that occasion. For Trial 19, M briefly touches unity but then falls sharply to about 0.6 and stays between 0.5 and 0.8 thereafter. The fall corresponds to a relatively sharp steepening of the ground-level concentration curve in Fig. 2. For this trial there is little further deterioration of the mass balance at the end.

In Trial 16, the mass balance is unusually poor, rising to nearly 1.7 in the early stages and then decreasing sharply. Reference to Fig. 1 suggests that the estimated mean ground-level concentration values are relatively high in the early part of this trial while the irregular behaviour at the end is due to difficulties in determining the height-scale (Fig. 3) when mean concentrations at the upper sensors were at times greater than those at ground level — in cases where the cloud profile could not be fitted the height and mass balance are recorded as zero.

For Trials 13, 11, 14 and 15, M briefly reaches a maximum near 1 but soon decreases again. At these low Richardson numbers concentrations are low and cloud heights grow rapidly thus making it difficult to detect all the gas.

In Trial 18, M oscillates around 0.65 and never exceeds 0.8. At early times, $\tau < 100$, this may be due to an underestimate of the area as the value extrapolated from the photographic analysis is used here, while the cloud envelope analysis implies areas twice as large [1]. The values of M do at least lend some support to these large values for cloud area.

3. Concluding remarks

In this paper we have sought to provide estimates of mean concentrations in the Thorney Island trials which are suitable for direct comparison with box-models of heavy gas dispersion.

We have found that the major parameter determining the nature of the dispersion is the initial Richardson number Ri_0, which expresses the relative importance of the influence of gravity and of atmospheric turbulence. After scaling time according to the gravity-spreading rate, we find that results show a very consistent variation with Ri_0.

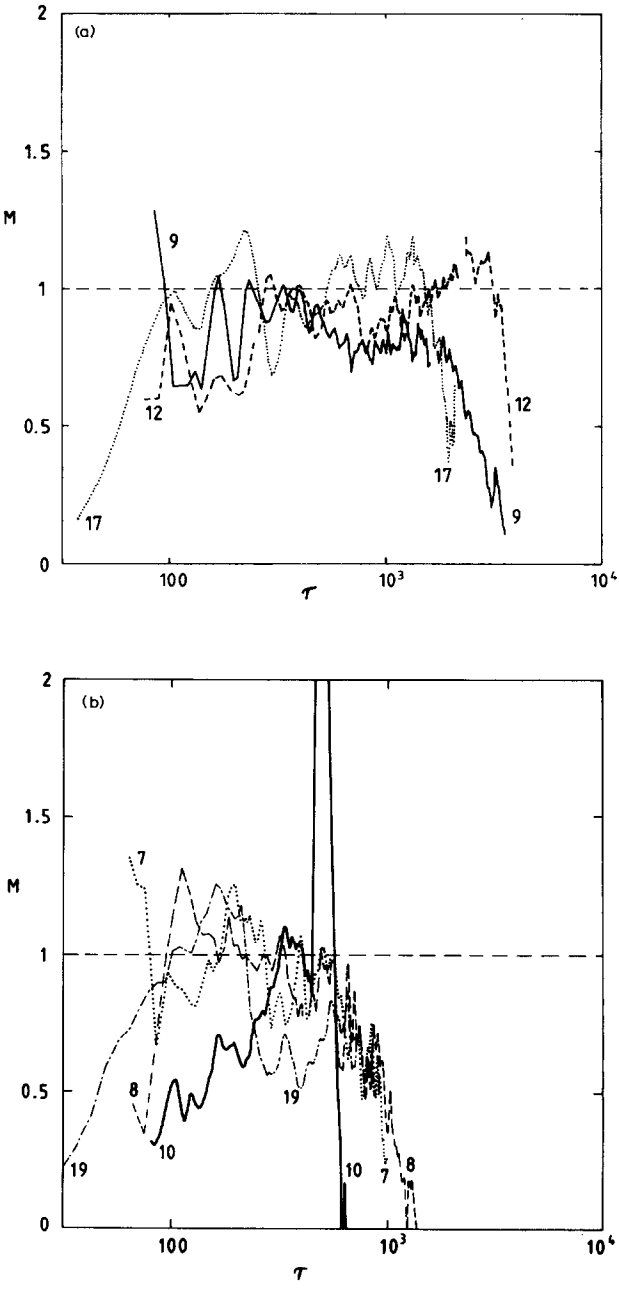

Fig. 5. Cloud mass balance, $M = A\int_0^\infty \bar{c}(z)dz/V_0c_0$, plotted against dimensionless time, τ. Calculated from mean concentrations smoothed over 15 seconds. Trial numbers indicated on graphs.

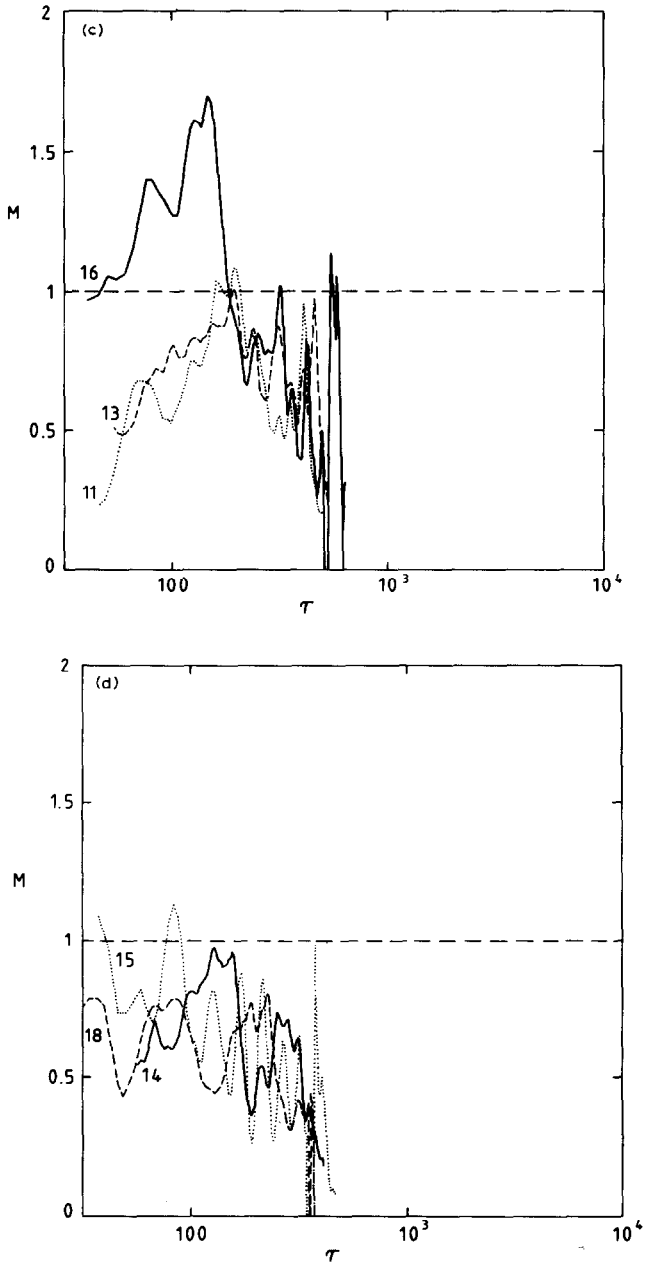

Fig. 5 (*Continued*).

The values of mean ground-level concentration $\bar{c}_g$ in Fig. 2 are consistent with a simple box-model in which the edge entrainment coefficient has a value of 0.7. It would be very interesting to know whether the simple de-

pendence of $\bar{c}_g$ holds in the long period (in logarithmic terms) between release and the arrival of the cloud at the first sensor mast. The complicated vortex-ring structure which develops in the cloud during this period [3] implies that the concentration distribution may well not be self-similar so that there is no particular reason to expect a simple behaviour of $\bar{c}_g$. Further light might be shed on this by determining the visual cloud height in the early stages and, for Trials 17—19, by examining data from the additional near-field ground-level gas detectors. Against these doubts may be set the behaviour of $\bar{c}_g$ in the high-Ri_0 trials when the edge entrainment relation appears to apply for very long periods.

The area-averaged concentration $\bar{c}_g$ does not match the ideal volume-averaged concentration which we defined in the Introduction. One difficulty in following that ideal procedure is that a definite cloud top cannot be determined from the concentration data. Whereas the edge of the cloud on the ground frequently meets the sensor masts as the cloud spreads and moves along providing a reasonable amount of data to trace its overall development [1], the vertical motion of the top of the cloud is monitored by only 4 levels of sensors and seems in any case to be dominated by small-scale fluctuations. The height-scale we have defined from the area-averaged concentrations does not in fact correspond to the cloud height defined in the Introduction. It could be brought closer to the ideal by using the fitted vertical profiles to find the height below which a certain proportion of the gas content of the cloud lies. However the height-scale has been used only to help assess the self-consistency of the results. It is not needed for matching to box model results since our mean concentration estimates appear more reliable.

Since the profiles of $\bar{c}(z)$ have been described for most of the time by a simple Gaussian curve, any definition of a volume-averaged concentration would in fact differ from $\bar{c}_g$ only by a constant multiple. However applying such a factor would spoil the consistency between the slope of the high-Ri_0 results in Fig. 2 with the initial release conditions.

To achieve a satisfactory match between the Thorney Island data and box models of heavy gas dispersion, it will be necessary to consider the reliability of the results as well as to resolve the above doubts about the behaviour at early times. The curves of Fig. 2 are based on a variable amount of data according to the number of masts in the cloud, and so greater errors are to be expected at the start and end of each curve. The evaluation of the mass balance and comparison with the graphs of other parameters gives clues to possible systematic errors related to the limit of sensitivity of the gas detectors. There are four principal ways in which this may have affected the results, all of which apply near the end of the data:

(i) The cloud outline used to determine A may be too small, as indicated by several of the curves in Fig. 8 of [1]. As discussed in Section 2.6 above, this does not seem to have a great effect on the mass balance. It would imply that the mean concentrations in the cloud will be overestimates because of the failure to sample low-concentration regions.

(ii) The results of Section 2.4 have indicated that there is a significant amount of gas remaining undetected in the upper part of the cloud. It is interesting to note that if a significant amount of gas is up there it is likely to be in an airstream moving considerably faster than the cloud below (see [1] for cloud speeds) and so it may form a dilute plume extending a considerable distance downwind of the main cloud. This process resembles the "detrainment" discussed by Wheatley and Webber [9].

(iii) As described in [1] for Trial 9 some gas may linger near the ground for a long time after the main body of the cloud has departed. Sometimes individual ground-level concentration records near the source take an abnormally long time to return to zero. Such tails have mostly been excluded from the horizontal averaging procedure described above and the departure time has been taken as the end of the main peak of the concentration record (see [6] for details of departure times used).

(iv) As the cloud leaves the sensor array the horizontal averaging samples only a region near the upwind edge, which presumbaly will lead to a systematic bias towards underestimates of $\bar{c}_g$. The time at which this starts might be estimated as when the centroid of the cloud leaves the array, which could be estimated from the results for cloud motion given in [1].

Acknowledgements

The work reported in this paper was performed on behalf of the Health and Safety Executive: I would like particularly to thank Dr J McQuaid for his cooperation and encouragement. However, the views expressed here are solely my own and do not necessarily reflect the views or the policy of the Health and Safety Executive.

References

1 P.W.M. Brighton, A.J. Prince and D.M. Webber, Determination of cloud area and path from visual and concentration records, J. Hazardous Materials, 11 (1985) 155—178.
2 R.G. Picknett, Dispersion of dense gas puffs released in the atmosphere at ground level, Atm. Environ., 15 (1981) 509—525.
3 J.W. Rottman, J.C.R. Hunt and A. Mercer, The initial and gravity-spreading phases of heavy gas dispersion: comparison of models with Phase I data, J. Hazardous Materials, 11 (1985) 261—279.
4 P.C. Chatwin, The use of statistics in describing and predicting the effects of dispersing gas clouds, J. Hazardous Materials, 6 (1982) 213—230.
5 C. Nussey, J.K.W. Davies and A. Mercer, The effect of averaging time on the statistical properties of sensor records, J. Hazardous Materials, 11 (1985) 125—153.
6 P.W.M. Brighton, Using concentration data to track clouds in the Thorney Island experiments, UKAEA Report, 1985 (in press).
7 M.J. Leck and D.J. Lowe, Development and performance of the gas sensor system, J. Hazardous Materials, 11 (1985) 65—89.
8 D.M. Webber, The physics of heavy gas clouds, UKAEA Report SRD R243, 1983.

9 C.J. Wheatley and D.M. Webber, Aspects of the dispersion of denser than air vapours that are of relevance to gas cloud explosions, Final Report of Contract between European Atomic Energy Community and UKAEA, EUR 9592en, 1984.
10 M.E. Davies and S. Singh, Thorney Island: its geography and meteorology, J. Hazardous Materials, 11 (1985) 91—124.
11 A.J. Prince, D.M. Webber and P.W.M. Brighton, Thorney Island Heavy Gas Dispersion Trials — determination of path and area of cloud from photographs, UKAEA Report SRD R318, 1985.
12 M.G. Kendall, Time-Series, Charles Griffin and Co, London, 2nd edn., 1976, pp. 29—31.